

EXPERIMENTS WITH A SPECTRAL CONVECTION MODEL

Hung-Chi Kuo

Department of Atmospheric Sciences
National Taiwan University, Taipei, Taiwan, R.O.C.

1. INTRODUCTION

With the progress of the computer and computational techniques, we have often experienced that the return to the first principles of physics enables a model to cope more easily with the complexity of the atmosphere. Ooyama (1990) propose a "primitive" form of moist thermodynamics. Instead of using pressure as a prognostic variable, Ooyama's model use the conservation of the entropy density, the momentum density and the total moisture density as predicted variables. When the hydrostatic approximation is made, the only change is how the vertical motion is computed (i.e., diagnostic instead of prognostic). Since the hydrostatic model has the physics of a GCM, we can run the two models in parallel and compare the "exact" physical results of the nonhydrostatic model with the various parameterizations formulated in the hydrostatic model. The advantage of the Ooyama's proposal is to give both accurate and consistent approaches to the reversible moist thermodynamic in a detailed, fine resolution, nonhydrostatic cloud model and a coarse resolution, hydrostatic (GCM-like) model. The only differences between the two models are spatial resolution and the way vertical motion is computed. The moist thermodynamics is identical. This allows us to analyze in detail what physics is lost (and hence needs to be parameterized) as model resolution coarsens and nonhydrostatic dynamics is replaced by hydrostatic dynamics.

The modeling studies reported here make use of a Fourier-Chebyshev spectral discretization of a nonhydrostatic model based on the "primitive" form of moist thermodynamics (Ooyama, 1990). Our goal is to employ a very *accurate* discretization on the model that has least assumptions in the moisture physics. We will use the model to study the interaction of radiative, convective and microphysical effects. We have constructed the convection model in two-dimension. The governing equations are presented in section 2. Section 3 gives the solution method. Numerical results are covered in section 4. Section 5 contains the concluding remarks.

2. GOVERNING EQUATIONS

Our modeling effort involves the Fourier-Chebyshev spectral discretization similar to that in Kuo and Schubert (1988) and the moist thermodynamics of the "primitive" form in Ooyama (1990). We believe a sound basis for moist thermodynamics and a accurate treatment of discretization are important for the improvement of cloud modeling.

The "primitive" form of moist thermodynamics makes model predictions strictly in terms of conservative properties, in particular the density of dry air ξ , density of total airborne moisture η , entropy density σ , the momentum densities $U = \rho u$, $V = \rho v$, $W = \rho w$, where $\rho = \xi + \eta$. The predicted values of ξ, η, σ at each spatial point are then input into a thermodynamic diagnosis, which outputs the temperature T and pressure p . Since, at any spatial point, $p = P(\xi, \eta, \sigma)$, we have $\nabla p = P_\xi \nabla \xi + P_\eta \nabla \eta + P_\sigma \nabla \sigma$. The P -coefficients are known functions of (ξ, η, σ) so that this formula for ∇p could now be used for the pressure gradient force in the momentum equations. However, Ooyama discussed how this can cause Gibbs' phenomena near cloud edges. As a solution he proposes weighted averages of the P -coefficients for saturated and unsaturated conditions. The overlap of the weighting coefficients is adjusted to the model spatial resolution.

We consider the two-dimensional (x, z) case described below. Here we have neglected frictional effects, but have included precipitation (or drizzle) effects in Q_η and radiative effects in Q_σ . The prognostic equations for the conservative variables are

$$\frac{\partial \xi}{\partial t} + \frac{\partial(\xi u)}{\partial x} + \frac{\partial(\xi w)}{\partial z} = 0, \quad (1)$$

$$\frac{\partial \eta}{\partial t} + \frac{\partial(\eta u)}{\partial x} + \frac{\partial(\eta w)}{\partial z} = Q_\eta, \quad (2)$$

$$\frac{\partial \sigma}{\partial t} + \frac{\partial(\sigma u)}{\partial x} + \frac{\partial(\sigma w)}{\partial z} = Q_\sigma, \quad (3)$$

$$\frac{\partial U}{\partial t} + \frac{\partial(Uu)}{\partial x} + \frac{\partial(Uw)}{\partial z} + \frac{\partial p}{\partial x} = 0, \quad (4)$$

$$\frac{\partial W}{\partial t} + \frac{\partial(Wu)}{\partial x} + \frac{\partial(Ww)}{\partial z} + g\rho + \frac{\partial p}{\partial z} = 0, \quad (5)$$

where

$$\rho = \xi + \eta, \quad u = \frac{U}{\rho}, \quad w = \frac{W}{\rho}. \quad (6, 7, 8)$$

The above constitute eight equations for the five prognostic variables ξ , η , σ , U , W , and the four diagnostic variables ρ , u , w and p . The system is closed by the thermodynamic diagnosis, the input of which is ξ , η , σ , and the output of which is temperature, pressure and the partition of η into its vapor and condensate parts. This requires writing two formulas (depending on whether the total airborne moisture η is entirely in the vapor phase or is partially condensed) for the entropy $\sigma(\xi, \eta, T)$, iteratively solving for two temperatures (T_1 and T_2) and then using

$$T = \max(T_1, T_2)$$

If $T_1 > T_2$ (unsaturated) $p_v = \eta R_v T$,

$$\eta_v = \eta, \quad \eta_c = 0$$

If $T_2 > T_1$ (saturated) $p_v = E(T)$,

$$\eta_v = \eta_*(T), \quad \eta_c = \eta - \eta_v$$

$$p_a = \xi R_a T, \quad p = p_a + p_v.$$

Here η_v and η_c are the densities of vapor and condensate respectively, p_a and p_v the partial pressures of dry air and water vapor respectively, $E(T)$ the saturation vapor pressure and η_* the mass density of saturated vapor.

Some points of the Ooyama's proposal worth noting are as follows.

1. The temperature and pressure are diagnostically determined from thermodynamics.

2. There is no need to predict water vapor and condensate separately; rather, they are diagnostically separated from the predicted total airborne water.

3. There is a modular separation of dynamics and thermodynamics; the link between dynamics and thermodynamics is through the pressure gradient force.

4. The discontinuity in thermodynamics due to phase change can be modified to a "gradual saturation" in order to make the moist ther-

modynamics match the spatial resolution of the model.

5. The ice phase can be handled by a hypothetical single phase condensate that behaves like liquid at warm temperatures, like ice at cold temperatures, with a gradual transition at intermediate temperatures.

6. When the hydrostatic approximation is made, the only change is how the vertical motion is computed, i.e., equation (5) is replaced by a simple diagnostic equation.

3. SOLUTION METHODS

The simulation of moist convections place great demands on spatial discretization schemes used in simulation models. In the present work we have used a scheme which is spectral in both horizontal directions. We shall solve the above system of equation on the domain $0 \leq x \leq L$, $0 \leq z \leq H$, with the assumption that all variables are periodic in x and $W = 0$ on $z = 0, H$. In the x direction, Fourier basis functions are used so that the periodicity is built into each basis function. In the z direction, Chebyshev polynomial basis functions are used; the top and bottom boundary conditions are not satisfied by each basis function, but rather by the series as a whole. In the following we discuss the spectral method for solving the above system.

The dependent variables (e.g. ξ) are approximated by the series expansions

$$\xi(x, y, t) = \sum_{m=-M}^M \sum_{n=0}^N \hat{\xi}_{mn}(t) T_n(z') e^{2\pi i m x / L} \quad (9)$$

where the $T_n(z')$ are the Chebyshev polynomials defined on the interval $-1 \leq z' \leq 1$ by $T_n(z') = \cos(n\phi)$ with $z' = 2z/H - 1 = \cos\phi$. Defining the Fourier-Chebyshev inner product of two functions $f(x, z)$ and $g(x, z)$ as

$$\langle f, g \rangle = \frac{1}{L} \int_{-1}^1 \int_0^L \frac{f(x, z) g^*(x, z)}{(1 - z'^2)^{1/2}} dx dz', \quad (10)$$

where the star denotes complex conjugate. The spectral coefficient $\hat{\xi}_{mn}(t)$ is given by

$$\hat{\xi}_{mn}(t) = \frac{2}{\pi c_n} \langle \xi(x, z, t), T_n(z') e^{2\pi i m x / L} \rangle \quad (11)$$

with $c_n = \begin{cases} 2 & n=0 \\ 1 & n>0 \end{cases}$. Equation (10) is the

transformation from physical space to Fourier-Chebyshev spectral space and (11) is the transformation back.

With the nonlinear terms defined by,

$$A = \xi u; \quad B = \xi w, \quad (12)$$

and to be computed by the transform method, the tau equation for ξ is

$$\frac{d\hat{\xi}_{mn}}{dt} + \hat{A}_{mn}^{(1,0)} + \hat{B}_{mn}^{(0,1)} = 0, \quad (13)$$

where $\hat{A}_{mn}^{(1,0)}$ is the spectral coefficients of $\partial A/\partial x$ and $\hat{B}_{mn}^{(0,1)}$ is the spectral coefficients of $\partial B/\partial z$. To eliminate aliasing error in the quadratic nonlinear terms, $3M$ points in x and $3N/2$ points in z are needed in the physical domain.

The relation between $\hat{A}_{mn}^{(1,0)}$ and \hat{A}_{mn} (the spectral coefficient of A) is

$$\hat{A}_{mn}^{(1,0)} = i \left(\frac{2\pi m}{L} \right) \hat{A}_{mn}, \quad (14)$$

while the relation between $\hat{B}_{mn}^{(0,1)}$ and \hat{B}_{mn} (the spectral coefficient of B) is

$$\hat{B}_{mn}^{(0,1)} = \frac{4}{Hc_n} \sum_{\substack{p=n+1 \\ p+n \text{ odd}}}^N p \hat{B}_{mp}. \quad (15)$$

Although the spectral evaluation of z derivatives by (15) looks at first sight more difficult than the spectral evaluation of x derivatives by (14), such is not the case. Equation (15) yields the (backward) recurrence formula

$$c_{n-1} \hat{B}_{m,n-1} - \hat{B}_{m,n+1} = \frac{4}{H} n \hat{B}_{m,n} \quad (n = 1, 2, \dots, N-1) \quad (16)$$

with the starting values $\hat{B}_{m,N+1} = \hat{B}_{m,N}^{(0,1)} = 0$. For fixed m , the use of (16) allows the N values of $\hat{B}_{mn}^{(0,1)}$ to be computed in $O(N)$ operations.

We have used the fourth-order Runge-Kutta scheme in the integration of (13). The $n = N-1, N$ modes of \hat{W} are solved from the boundary conditions ($W = 0$). Details of the discretization can be found in Kuo and Schubert (1988).

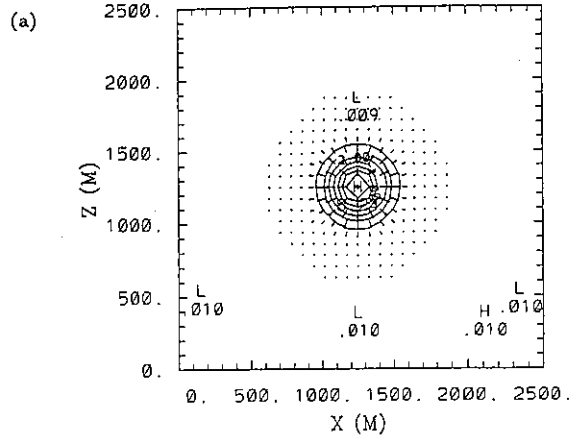
4. NUMERICAL RESULTS

We have used $L = H = 2500m$, $M = 16$, $N = 32$ and $\Delta t = 0.075s$ in our calculation. In addition, the Lanczos filter has applied to the tendency of the spectral variables. We present a dry hydrostatic adjustment experiment in our paper.

The basic states used are $\bar{\eta} = 0$,

$$\bar{T}(z) = 293.15 - g/R_d z,$$

U, W & σ' 0.30 sec



ξ' 0.30 sec

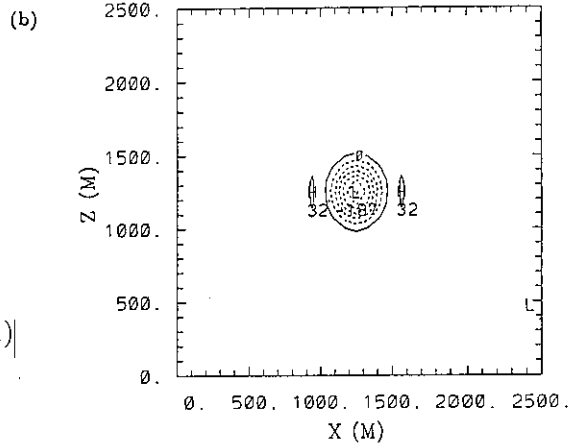


Figure 1 The U, W, σ' and ξ' (dry air density) in physical domain at time 0.3 second for the calculation with $\Delta T = 2.5K$. The peak momentum is $0.756 \text{ kgm}^{-2} \text{ s}^{-1}$ and the contour interval for σ is $1 \text{ Jm}^{-3} \text{ K}^{-1}$. The contour interval for ξ is $3 \times 10^{-3} \text{ kgm}^{-3}$ and the unit is 10^{-5} kgm^{-3} .

and

$$\bar{\xi}(z) = 1.1478 \text{kgm}^{-3}.$$

The basic states satisfy the hydrostatic balance. Superimpose on the basic state is a T' anomaly defined as

$$T' = \Delta T \exp\left(-\left(\frac{x-1250}{200}\right)^2\right) \exp\left(-\left(\frac{z-1250}{200}\right)^2\right).$$

We have also set the ξ' equal to zero in our initial condition. Thus only the p' and σ' anomaly exist along with the T' anomaly. Since $\xi' = 0$, the anomaly (bubble) has no buoyancy and will not rise. Moreover, hydrostatic balance is violated with $\xi' = 0$.

Figure 1 shows the U, W, σ' and ξ' in physical domain at time $0.3s$ for the calculation with $\Delta T = 2.5K$. Figures 2 and 3 are similar to Figure 1 except at time $1.8s$ and $30s$ respectively. Figure 3 reveals the motion and density fields associated with a rising bubble. This rising bubble (now $\xi' < 0$) can be viewed as the result of the hydrostatic adjustment by the acoustic waves. In contrast, Figures 1 and 2 indicate the motions and density fields associated with the acoustic wave transient.

To see how fast the acoustic wave can make the hydrostatic adjustment, we have plot the time series at the center of the domain for the variables of divergence, T' , ξ' and p' in Figure 4. It takes about 3 to 4 seconds for these variables to reach a steady state. Figure 5 is similar to Figure 4 except for $\Delta T = 7.5K$ case. Interestingly, the time series in both cases are very similar. This indicates the atmosphere reaches the "anelastic balance" ($\partial p' / \partial t \approx 0$) or converts a zero ξ' to a finite value of ξ' in 3 to 4 seconds regardless of the size of ΔT . Discussions about the one-dimensional acoustic adjustment with a isothermal basic state can be found in Bannon (1995).

5. CONCLUDING REMARKS

We have constructed a new spectral convection model that employ the least assumptions in the moist physics. This reformulated model will be used to study the interaction of radiative, convective, and drizzle effects. We are currently improving the efficiency of time discretization. Preliminary results from the model will be given in the conference.

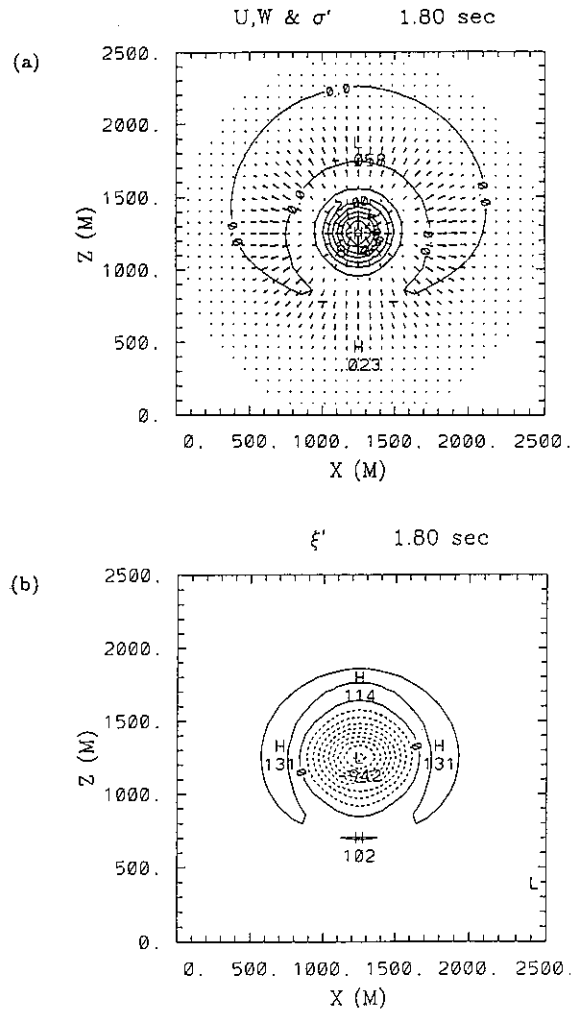


Figure 2 Similar to Figure 1 except at time 1.8 second. The peak momentum is $0.61 \text{kgm}^{-2}\text{s}^{-1}$ and the contour interval for σ is $1 \text{Jm}^{-3}\text{K}^{-1}$. The contour interval for ξ is $3 \times 10^{-4} \text{kgm}^{-3}$ and the unit is 10^{-5}kgm^{-3} .

REFERENCES

- Bannon, P. R., 1995: Hydrostatic adjustment: Lamb's problem. *J. Atmos. Sci.*, **52**, 1743-1752.
- Kuo, H.-C., and W. H. Schubert, 1988: Stability of cloud-topped boundary layers. *Quart. J. R. Meteor. Soc.*, **114**, 887-916.
- Ooyama, K. V., 1990: A thermodynamic foundation for modeling the moist atmosphere. *J. Atmos. Sci.*, **47**, 2580-2593.

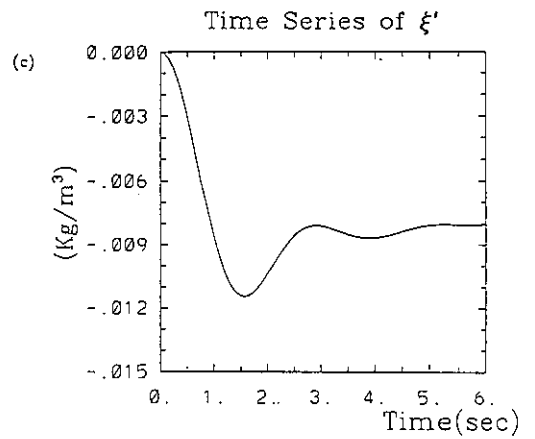
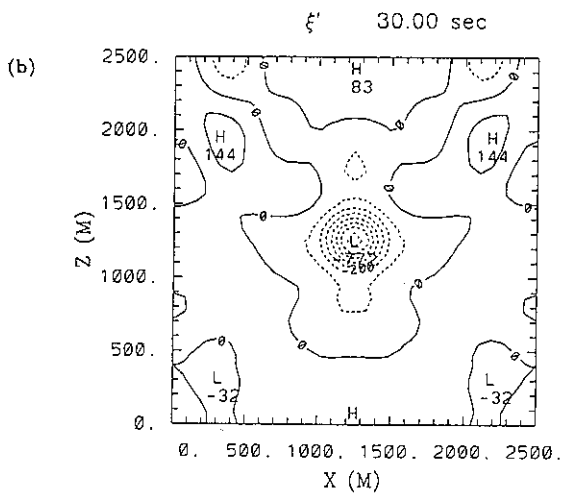
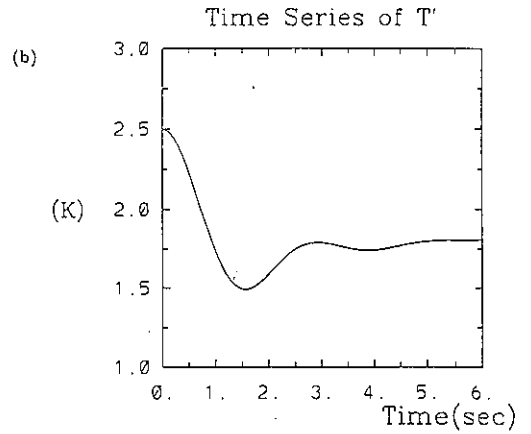
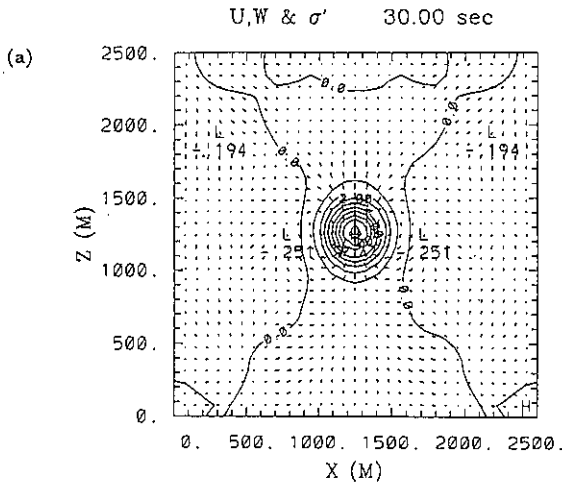


Figure 3 Similar to Figure 1 except at time 30 second. The peak momentum is $1 \text{ kgm}^{-2} \text{ s}^{-1}$ and the contour interval for σ is $1 \text{ Jm}^{-3} \text{ K}^{-1}$. The contour interval for ξ is $3 \times 10^{-4} \text{ kgm}^{-3}$ and the unit is 10^{-5} kgm^{-3} .

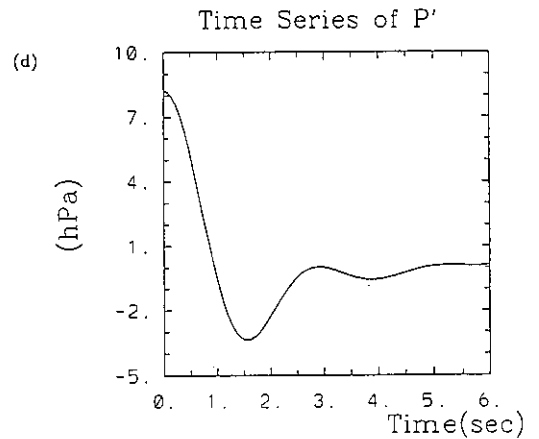
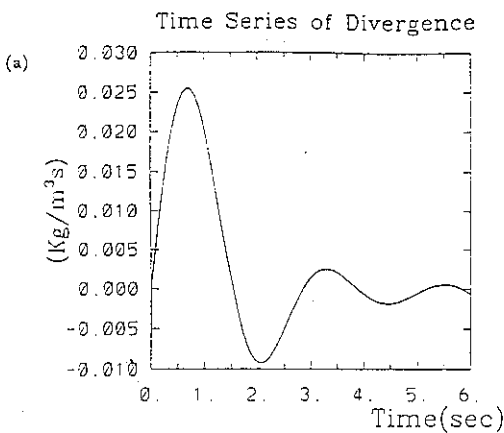
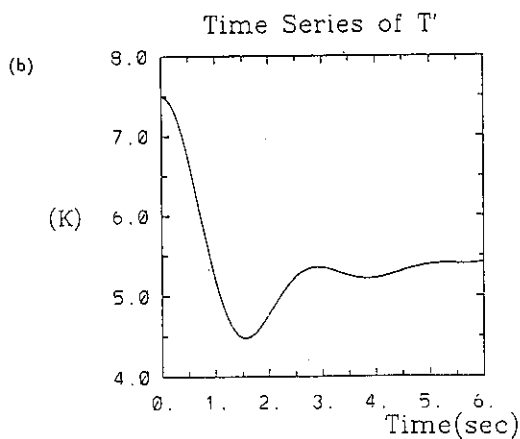
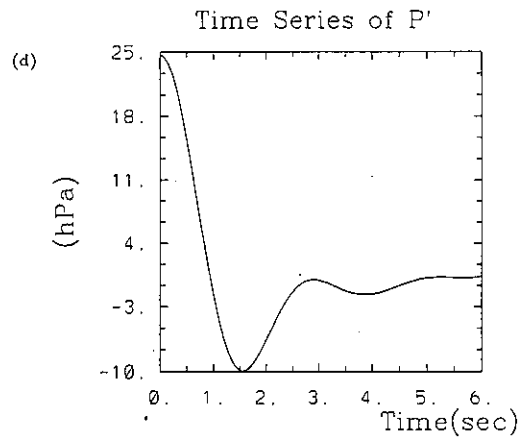
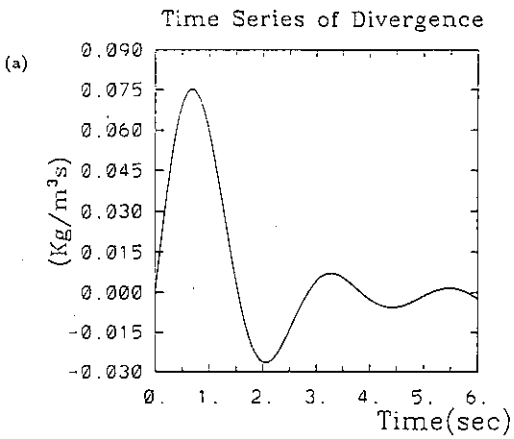


Figure 4 The time series at the center of the domain for the variables of momentum density divergence, T' , ξ' and p' for the experiment with $\Delta T = 2.5 \text{ K}$.



ACKNOWLEDGMENT

This research was supported by the Grants NSC 85-2111-M002-007AP1 from the National Research Council of Taiwan.

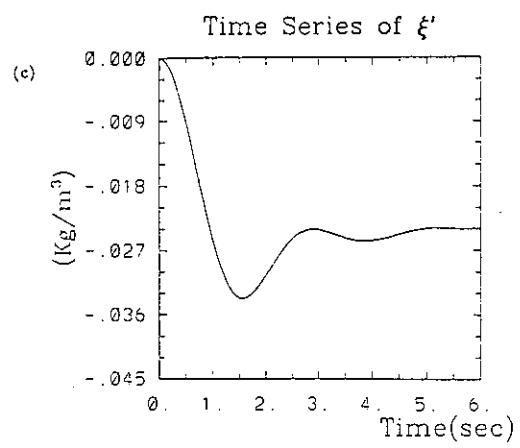


Figure 5 Similar to Figure 4 except for the experiment with $\Delta T = 7.5K$.